Simplified Fluid-Structure Interactions for Hemodynamics

Olivier Pironneau

Abstract Computing blood flows in a closed vascular system by isolating one section for simulation creates instabilities due to the time-periodic structure of the flow and possible non-physical back flow in the simplified geometry. We propose some solutions in the context of a simplified fluid structure interaction on a fixed geometry but with pressure dependent normal velocities at the compliant walls.The present analysis is based on the Surface Pressure model for the fluid-structure interactions.

Keywords Blood flow · Hemodynamics finite element method · Pressure boundary conditions · Primary: 91B28, 65L60 · Secondary: 82B31

1 Introduction

Mastering the simulation of blood flow is the key to proper design of by-passes, stents and heart valves (see Thiriet [17] for instance).

The problem was addressed by Charles Peskin in the nineties and his team have made impressive simulations since, using fictitious domains and immersed boundary techniques [1, 12, 13, 18].

Another approach, taken by Quarteroni et al. [5] and the REO project at INRIA [3, 4, 19] is to discretize the full fluid-structure coupled problem with solvers working in moving domains.

In a seminal paper [11], Nobile and Vergana showed that the problem is well posed and conserves energy. Nevertheless the numerical simulations are expensive [2] and there is room for simplifications.

O. Pironneau (✉)
Laboratoire Jacques-Louis Lions, Sorbonne Universités, UPMC,
Boite courrier 187, 75252 Paris Cedex 05, France
e-mail: olivier.pironneau@upmc.fr

S. R. Idelsohn (ed.), *Numerical Simulations of Coupled Problems in Engineering*,
Computational Methods in Applied Sciences 33, DOI: 10.1007/978-3-319-06136-8_3,

In the special case of aortic flow the geometry does not change much. Typically the aorta has a radius of 1cm and a computational geometry deals with a section of length of 5–10 cm; the thickness of the aortic wall is around 0.1 cm; the heart pulse is about 1 Hz and the pressure drop roughly 6 KPa.

In principle arteries are deformable solids subject to large displacements and nonlinear elasticity (e.g. [7, 8, 10]). But when small displacement occurs only and linear elasticity applies, shell models like Koiter's can be used. It was shown in [11] that if lateral displacements are neglected, Koiter's model reduces to a scalar equation for the normal displacement η

$$\rho^s h\partial_{tt}\eta - \nabla\cdot(\mathbf{T}\nabla\eta) - \nabla\cdot(\mathbf{C}\nabla\partial_t\eta) + a\partial_t\eta + b\eta = f^s,\ \eta, \partial_t\eta \text{ given at } t=0 \tag{1}$$

on the mean position Σ of the vessel's wall; here h denotes the average thickness of the vessel and ρ^s its volumic mass; $\mathbf{T}$ is the pre-stress tensor (needed because at rest the vessel is blown up by the blood); $\mathbf{C}$ is a damping term, a, b are viscoelastic terms and f^s the external normal force, i.e. $-\sigma^{\mathbf{s}}{}_{nn}$ the normal component of the normal stress at the surface of the solid.

Notice however that the other components of the normal stress tensor cannot be matched with the fluid when the displacement is assumed normal.

Finally assume that $[h, T, C, a] << b$; then the *Surface Pressure Model* is obtained:

$$-\sigma^{\mathbf{s}}{}_{nn} = b\eta, \text{ with } b = \frac{Eh\pi}{A(1-\xi^2)} \tag{2}$$

where A is the vessel's cross section, E the Young modulus, ξ the Poisson coefficient. Some typical values (MKSA):

$$E = 3MPa,\ \xi = 0.3,\ A = \pi R^2,\ R = 0.01,\ h = 0.001,\ \Rightarrow\ b = 3.310^7 \mathrm{ms}^{-2} \tag{3}$$

2 Boundary Conditions

With simple toroidal coordinates $(r,\theta,\phi) \to (x = R\cos\phi,\ y = R\sin\phi,\ z = r\sin\theta)$ where $R = R_0 + r\cos\theta$,

$$\nabla\cdot u = h_r h_\theta h_\phi \left(\partial_r \frac{u_r}{h_\theta h_\phi} + \partial_\theta \frac{u_\theta}{h_\phi h_r} + \partial_\phi \frac{u_\phi}{h_r h_\theta}\right) \tag{4}$$

with $h_r = 1,\ h_\theta = \frac{1}{r},\ h_\phi = \frac{1}{R}$ because, by definition

$$\frac{1}{h_k^2} = (\partial_k x)^2 + (\partial_k y)^2 + (\partial_k z)^2, \quad k = r, \theta, \phi \tag{5}$$

So $\nabla \cdot u = 0$ and $u \times n = 0$ imply

$$\nabla \cdot u = \partial_r u_r + u_r \frac{R_0 + 2r\cos\theta}{r(R_0 + r\cos\theta)} = 0 \Rightarrow \partial_r u_r|_{\partial\Omega} = -\frac{u_r}{r}\frac{R_0 + 2r\cos\theta}{R_0 + r\cos\theta} \tag{6}$$

Similarly

$$\nabla u = \sum_i e^i h_i \otimes \partial_k \left(\sum_k e^k u_k \right), \quad i, k \in (r, \theta, \phi) \tag{7}$$

with

$$\begin{aligned} e^r &= (\cos\theta\cos\phi, \cos\theta\sin\phi, \sin\theta)^T, \\ e^\theta &= (-\sin\theta\cos\phi, -sin\theta\sin\phi, \cos\theta)^T, \quad e^\phi = (-\sin\phi, \cos\phi, 0)^T \end{aligned} \tag{8}$$

Thus

$$n^T(\nabla u)n = \partial_r u_r + \frac{u_r}{r}\left(1 + \frac{r}{R}\cos^2\theta\right) \Rightarrow \sigma_{nn}^f = p + 2\left(1 + \frac{r}{R}\cos^2\theta\right)\frac{\mu}{r}u \cdot n. \tag{9}$$

Hence the matching conditions at the fluid-structure interface on a torus of small radius r and big radius R are

$$\partial_t \eta = u \cdot n, \quad p = 2\left(1 + \frac{r}{R}\cos^2\theta\right)\frac{\mu}{r}\partial_t \eta + b\eta \tag{10}$$

Notice that (10) implies

$$\partial_t p = 2\left(1 + \frac{r}{R}\cos^2\theta\right)\frac{\mu}{r}\partial_t u \cdot n + bu \cdot n \tag{11}$$

3 Moving Fluid Domains Versus Fixed Domains

3.1 Energy Considerations

Assuming the fluid Newtonian and incompressible, the pressure p and the velocity u are given by the Navier-Stokes equations

$$\rho^f\left(\frac{\partial u}{\partial t} + u \cdot \nabla u\right) - \nabla \cdot \sigma^f = 0, \quad \nabla \cdot u = 0, \tag{12}$$

where ρ^f is the volumic mass of the fluid, μ the viscosity and $\sigma^f = -p\mathbf{I} + \mu(\nabla u + \nabla u^T)$ is the stress tensor.

To check the energy budget one multiplies (12) by u and integrates by parts:

$$\int_\Omega \left[\frac{\rho^f}{2}\partial_t|u|^2 + \frac{\mu}{2}(\nabla u + \nabla u^T) : (\nabla u + \nabla u^T)\right] + \int_{\partial\Omega} \frac{\rho^f}{2}|u|^2 u \cdot n = \int_{\partial\Omega} \sigma^s \cdot u \cdot n \tag{13}$$

The fluid velocity on $\partial\Omega$ is equal to the wall velocity, so (see [5])

$$\int_{\Omega(t)} \frac{1}{2}\partial_t|u|^2 + \int_{\partial\Omega} \frac{1}{2}|u|^2 u \cdot n = \partial_t \int_{\Omega(t)} \frac{1}{2}|u|^2 \tag{14}$$

This leads to the following energy identity

$$\int_{\Omega(T)} \frac{\rho^f}{2}|u|^2(T) + \int_{\Omega\times(0,T)} \frac{\mu}{2}|\nabla u + \nabla u^T|^2 = \int_{\Omega(0)} \frac{\rho^f}{2}|u|^2(0) + \int_{\partial\Omega\times(0,T)} \sigma^s \cdot u \cdot n \tag{15}$$

3.2 The Problem in Strong Form

Now if we consider (12) on a fixed domain with zero tangential velocities but non-zero normal velocities on the walls then to conserve energy we need to change $u \cdot \nabla u$ into $u \cdot \nabla u - \frac{1}{2}\nabla|u|^2$ which happens to be $-u \times \nabla \times u$ due to the identity

$$u \cdot \nabla u = \frac{1}{2}\nabla|u|^2 - u \times \nabla \times u. \tag{16}$$

Let us recall another identity:

$$-\Delta u = \nabla \times \nabla \times u + \nabla\nabla \cdot u \tag{17}$$

Therefore the modified Navier-Stokes system suited to flows in fixed domains with zero tangential components on the walls ($u \times n = 0$) is

$$\rho^f\left(\frac{\partial u}{\partial t} - u \times \nabla \times u\right) + \mu\nabla \times \nabla \times u + \nabla p = 0, \quad \nabla \cdot u = 0, \tag{18}$$

In a domain Ω with $u \cdot n = 0$ and p related by (11) on $\partial\Omega$, as shown below.

3.3 The Problem in Variational Form

Its variational formulation of is: find u, p such that $\forall \hat{u}$, $\hat{p}$ with $\hat{u} \times n|_{\partial\Omega} = 0$,

$$\int_\Omega \left[\rho^f \left(\frac{\partial u}{\partial t} - u \times \nabla \times u \right) \cdot \hat{u} + \mu \nabla \times u \cdot \nabla \times \hat{u} - p \nabla \cdot \hat{u} - \hat{p} \nabla \cdot u \right] + \int_{\partial\Omega} p \hat{u} \cdot n = 0. \tag{19}$$

with p related to $u \cdot n$ by (11).

Problem 1 Find u, p, η such that $\forall \hat{u}$, $\hat{p}$, $\hat{\eta}$ with $\hat{u} \times n|_{\partial\Omega} = 0$, u and η given at $t = 0$,

$$\int_\Omega [\rho^f \left(\frac{\partial u}{\partial t} - u \times \nabla \times u \right) \cdot \hat{u} + \mu \nabla \times u \cdot \nabla \times \hat{u} - p \nabla \cdot \hat{u} - \hat{p} \nabla \cdot u] + \int_{\partial\Omega} [(\alpha \partial_t \eta + b\eta) \hat{u} \cdot n + b\hat{\eta}(\partial_t \eta - u \cdot n)] = 0. \tag{20}$$

with $\alpha = 2\frac{\mu}{r}\left(1 + \frac{r}{R}\cos^2\theta\right)$. As (20) implies (10-a),
energy estimates derive by choosing $\hat{u} = u$, $\hat{p} = p$, $\hat{\eta} = \eta$

$$\int_\Omega \rho^f |u|^2(T) + \int_{\partial\Omega} b\eta^2(T) + \int_{\Omega\times(0,T)} 2\mu |\nabla \times u|^2 + 2 \int_{\partial\Omega\times(0,T)} \alpha (\partial_t \eta)^2 = \int_\Omega \rho^f |u|^2(0) + \int_{\partial\Omega} b\eta^2(0) \tag{21}$$

3.4 Approximation with the Nedelec Edge Element

Boundary conditions like $u \times n$ are hard to enforce. Furthermore boundary conditions involving the pressure have their own difficulties (see [15, 16]). In [6] it is argued that finite element approximations of (24) requires edge elements. An error analysis is given with $P^k - P^{k-1}$ discontinuous elements with degrees of freedom being edge fluxes of degree k plus face fluxes of degree $k-1$ and volume fluxes of degree $k-2$ for the velocities.

Although the proof of convergence is done for $k \geq 2$, we tested the same idea with P^1 Raviart-Thomas elements (called RT^0) for the velocity and P^0 discontinuous elements for the pressure. In theory η should be P^0-discontinuous like the pressure; first we took it P^1-continuous to simplify the implementation because then we can

add to the formulation a small regularization $-\epsilon\Delta\eta$ everywhere in Ω so as to avoid having degrees of freedom for η only on the boundary.

Then we tested also η approximated with the P^1 Raviart-Thomas element and formulated the laplacian of η in mixed form; this augments considerably the number of degree of freedom: $3*(n_v+n_e)+2*n_v$ for the $P^2-P^1-P^1$ element (tested in [14], see also below), $3*n_e+n_t+2*n_v$ for the $RT^0-P^1-P^1$ element and $6*n_e+2*n_t+2*n_v$ for the $RT^0-P^0-RT^0+P^0$ element, where n_v is the number of vertices, n_e the number of edges, n_t the number of elements. We tested these 3 sets of element on a simple geometry: a quarter of a torus with a pressure drop imposed from the top horizontal cross section to the right vertical one. The cross section of the torus is a circle of radius 1 cm. This circle is extruded on a greater circle of radius 4 cm. The pressure drop is $6\cos(\pi t)$, $b=200$ and $\nu=0.001$.

The time step is 0.05. The mesh has $n_v=1395$, $n_t=6120$, $n_e=1336$. The computation is stopped at $t=0.75$.

The results are shown on Fig. 4. On a core i7@2.3MHz it takes 17 s with the Nedelec-P^1-P^1 element to compute 16 time steps with the characteristic-Galerkin method for the non-linear terms (see [14]) and 22 s with the Nedelec/Raviart-Thomas element (see Fig. 1).

4 A Formulation Where the Displacement is Eliminated

Notice that η can be eliminated from (10), giving a formulation which contains $u\times n=0$ and

$$n\partial_t p=\alpha\partial_t u+bu \tag{22}$$

4.1 A Time Discretisation

Consider now (19) discretized in time :

$$\int_\Omega\left[\rho^f\left(\frac{u^{m+1}-u^m}{\delta t}-u^{m+\frac12}\times\nabla\times u^m\right)\cdot\hat u+\mu\nabla\times u^{m+\frac12}\cdot\nabla\times\hat u-p^{m+1}\nabla\cdot\hat u\right.$$
$$\left.-\hat p\nabla\cdot u^{m+\frac12}\right]+\int_{\partial\Omega}p^{m+1}\hat u\cdot n=0. \tag{23}$$

We use (22) discretized in time to compute $p^{m+1}|_{\partial\Omega}$ and so we consider

Problem 2 Find u, p such that $\forall\hat u$, $\hat p$ with u and $\partial_t p$ given at $t=0$,

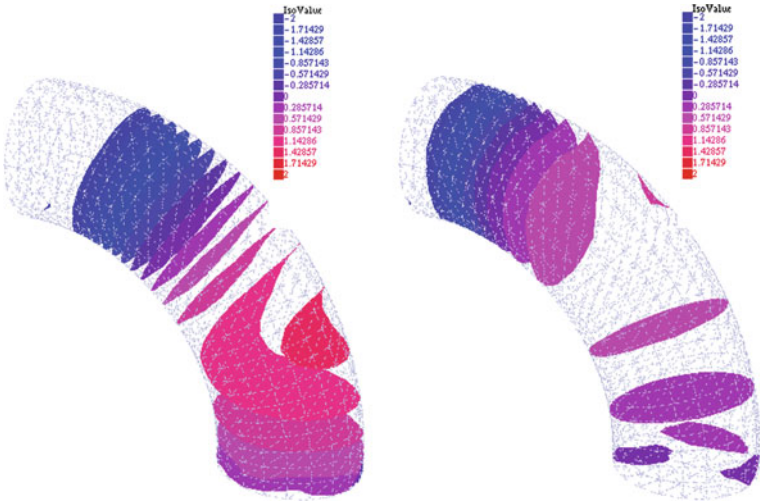

Fig. 1 *Left* Surfaces of constant pressure for a flow with $\nu = 10^{-3}$, $b = 200$ in a quarter of a torus with $R = 4$, $r = 2$ discretized on a fixed geometry with the Nedelec edge element for the velocity, peacewise constant pressures and linear continuous deformation. *Right* same as *left* but with a mixte Raviart-Thomas element for the displacement

$$\int_\Omega \left[\rho^f \left(\frac{u^{m+1} - u^m}{\delta t} - u^{m+\frac{1}{2}} \times \nabla \times u^m \right) \cdot \hat{u} + \mu \nabla \times u^{m+\frac{1}{2}} \cdot \nabla \times \hat{u} - p^{m+1} \nabla \cdot \hat{u} \right.$$
$$\left. - \hat{p} \nabla \cdot u^{m+\frac{1}{2}} \right] + \int_{\partial\Omega} [\delta t b u^{m+\frac{1}{2}} + \alpha (u^{m+1} - u^m) + p^m n] \cdot \hat{u} = 0. \tag{24}$$

Formulation (19) is valid only if $\hat{u} \times n = 0$. This condition has been removed from (24) to make it symmetric and easy to implement but the consequence is that by working the integrations by parts backward, it is found that this formulation implies (18) and on $\partial\Omega$:

$$[\delta t b u^{m+\frac{1}{2}} + \alpha (u^{m+1} - u^m)] \cdot n - (p^{m+1} - p^m), \qquad \nabla \times u^{m+\frac{1}{2}} \times n = 0 \tag{25}$$

The first condition no longer implies that $u \times n = 0$ and the second condition is like saying that the tangential stress is zero, which means that we match not only the normal components of the fluid and solid normal stress but all the components.

In summary Problem 2 is different from Problem 1; both of them have physically sound background but we need to test them numerically to see how different they are.

4.2 Discretization with a Finite Element Method

Let T_h be a triangulation with K tetraedra $\{T_k\}_1^K$ with the usual conformity hypotheses; let $\Omega := \cup_k T_k \subset \mathbb{R}^3$.

Consider the $P^2 - P^1$ element built from

$$\begin{aligned} V_h &= \{v \in C^0(\overline{\Omega})^3 \ : \ v_i|_{T_k} \in P^2, \ i = 1, 2, 3\} \\ Q_h &= \{q \in C^0(\overline{\Omega}) \ : \ q|_{T_k} \in P^1\} \end{aligned} \tag{26}$$

We assume that the boundary is made of two part, Σ which is the compliant wall and the input and output sections Γ on which p is given and $u \times n = 0$.

4.3 Discretization of Problem 1

For simplicity we assume that $r << R$, i.e. $\alpha = 1$. The momentum equation is also divided by ρ^f and $\nu = \mu/\rho^f$ and b is changed into b/ρ^f.

A feasible discretization of (24) is to find $[u^{m+1}, p^{m+1}, \eta^{m+1}] \in V_h \times Q_h \times Q_h$ with $u^{m+1} \times n|_\Gamma = 0$, $\eta^{m+1}|_\Gamma = 0$ and such that

$$\begin{aligned} &\int_\Omega \left[\hat{u} \cdot \left(\frac{u^{m+1} - u^m}{\delta t} - u^{m+\frac{1}{2}} \times \nabla \times u^m \right) - p^{m+1} \nabla \cdot \hat{u} - \hat{p} \nabla \cdot u^{m+\frac{1}{2}} \right] \\ &\quad + \int_\Omega \nu \nabla \times u^{m+\frac{1}{2}} \cdot \nabla \times \hat{u} + \varepsilon \nabla \eta^{m+\frac{1}{2}} \cdot \nabla \hat{\eta}] \\ &\quad + \int_\Sigma b \left[\eta^{m+\frac{1}{2}} \hat{u}_n - \hat{\eta} \left(u_n^{m+\frac{1}{2}} - \frac{1}{\delta t}(\eta^{m+1} - \eta^m) \right) + \frac{1}{\epsilon}(u^{m+\frac{1}{2}} \times n) \cdot (\hat{u} \times n) \right] \\ &= - \int_\Gamma p_\Gamma \hat{u}_n, \quad \forall \, [\hat{u}, \hat{p}, \hat{\eta}] \in V_h \times Q_h \times Q_h \text{ with } \hat{u} \times n|_\Gamma = 0, \ \hat{\eta}|_\Gamma = 0. \end{aligned} \tag{27}$$

where ε is any small positive parameter.

When Ω is kept fixed, an energy consevation identity is found by choosing $\hat{u} = u^{m+\frac{1}{2}}$, $\hat{p} = -p^{m+1}$, $\hat{\eta} = \eta^{m+\frac{1}{2}}$:

$$\begin{aligned} &\int_\Omega \left[\frac{u^{m+1\,2} - u^{m\,2}}{\delta t} + \nu |\nabla \times u^{m+\frac{1}{2}}|^2 + \varepsilon |\nabla \eta^{m+\frac{1}{2}}|^2 \right] \\ &\quad + \int_\Sigma \frac{\eta^{m+1\,2} - \eta^{m\,2}}{\delta t} + \frac{1}{\epsilon} \int_\Sigma |u^{m+\frac{1}{2}} \times n|^2 = - \int_\Gamma p_\Gamma \hat{u}_n^{m+\frac{1}{2}} \end{aligned} \tag{28}$$

As for the Navier-Stokes equations, when δt is small enough the problem has a unique solution because of the energy estimate and because of a general inf-sup condition is satisfied with p replaced by $[p, \eta]$.

4.4 Discretization of Problem 2

A feasible discretization of (24) is to find $u^{m+1} \in V_h,\ p^{m+1} \in Q_h$ such that

$$\begin{aligned}
&\int_\Omega \left[\hat{u} \cdot \left(\frac{u^{m+1} - u^m}{\delta t} - u^{m+\frac{1}{2}} \times \nabla \times u^m \right) - p^{m+1} \nabla \cdot \hat{u} - \hat{p} \nabla \cdot u^{m+\frac{1}{2}} \right] \\
&\quad + \int_\Omega \nu \nabla \times u^{m+\frac{1}{2}} \cdot \nabla \times \hat{u} \\
&\quad + \int_\Sigma (u^{m+\frac{1}{2}} b \delta t + p^m n) \cdot \hat{u} = - \int_\Gamma p_\Gamma \hat{u}_n \\
&\forall \hat{u} \in V_h, \hat{p} \in Q_h \text{ with } \hat{u} \times n|_\Gamma = 0
\end{aligned} \tag{29}$$

Notice that $u^{m+1} \times n|_\Sigma = 0$ is implied by the formulation. When Γ is flat that condition amounts to some component of the velocity being zero which is easy to implement.

Notice that the energy equality implies stability only so long a p remains bounded on Σ, which could possibly be derived from (29), but not so obviously:

$$\begin{aligned}
&\int_\Omega \left[\frac{u^{m+1\,2} - u^{m\,2}}{\delta t} + \nu |\nabla \times u^{m+\frac{1}{2}}|^2 \right] + \int_\Sigma b |u^{m+\frac{1}{2}}|^2 \delta t \\
&\qquad = - \int_\Sigma p^m u_n^{m+\frac{1}{2}} - \int_\Gamma p_\Gamma \hat{u}_n^{m+\frac{1}{2}}
\end{aligned} \tag{30}$$

5 Numerical Tests

5.1 Moving the Geometry for Graphic Visualization

The full model requires that Σ be moved at every time step along its normal of a quantity $\delta t u^m \cdot n$. To preserve the triangulation we follow the literature [2] and solve an additional problem

$$-\Delta d^{m+1} = 0 \text{ in } \Omega,\ \ d^{m+1}|_\Sigma = d^m + n \delta t u_n^m,\ \ d^{m+1}|_\Gamma = 0 \tag{31}$$

and then move every vertex q^j of the triangulation $q^j \to q^j + \kappa d$. In theory $\kappa = 1$ but for graphic enhancement it can be adjusted. Note however that (31) is expensive.

5.2 Comparison of the Two Methods

On the problem described earlier both methods give very similar results as shown on Fig. 2. The geometry is updated for visualisation purpose with a multiplicative factor 100.

The geometry is a section of the aorta obtained from a MRI scan. It has 4991 vertices, giving 19964 degrees of freedom for each linear systems for $[u_1^{m+1}, u_2^{m+1}, u_3^{m+1}, p^{m+1}]$. The pressure drop from inflow section on the right to outflow section on the left is $p_{\Gamma_R} = 6\cos^2(\pi t)$ and the results are shown at $t = 0.8$. On the smaller cross sections a pressure drop equal to $p_{\Gamma_R}/2$ is imposed. Problem 1 and Problem 2 are solved for comparison with $\delta t = 0.05/\pi,\ \nu = 0.001,\ b = 200$. Results are shown on Fig. 3.

For Problem 1, the computation took 198″ on a macbook pro 15″, 2012, 2.3MHz core i7. For Problem 2 it took 180″. The results are very similar with some difference on the pressure but very little on the velocities.

6 Inflow/Outflow Conditions by PML

We end this article with an idea to address the problem of loss of stability due to the creation of reverse flow in unwanted regions because of the boundary conditions on the artificial inflow and out flow sections.

We borrow the idea from the PML literature (see for example [9]) and add to the artery geometry a viscous buffer after Γ_{out} where $\nu = \nu_1 >> \nu_{blood}$ (and similarly before Γ_{in} but we present the theory applied to the outflow section only).

Consider a geometry Ω where the exit section is $\Gamma_o = \{0\} \times [0, h]$ in 2D where pressure is set to p_0 while pressure is set to p_1 on entry. Assume that we impose a parabolic flow $u = Ky(h - y)$ at the exit of a viscous buffer $\mathbf{L} = [-L, 0) \times [0, h]$, i.e. on $\{-L\} \times [0, h]$. Now we solve the Navier-Stokes equations on $\Omega \cup \mathbf{L}$. The problem is to choose K so that the pressure on the inital outflow boundary Γ_o is unchanged in the mean, namely $\bar{p}_0 := h^{-1} \int p_0 \mathrm{d}y$.

Because at every time step the system to solve is linear we shall adjust K by superposition so that the mean pressure is $\bar{p}_0$ on Γ_{out}. Since, $p|_{\Gamma_{out}} \approx \bar{p}_1 + (\bar{p}_2 - \bar{p}_1)\frac{K-K_1}{K_2-K_1}$ where $\bar{p}_1$ is computed with $K = K_1$ and $\bar{p}_2$ the mean pressure when $K = K_2$, then

$$K = K_1 + (K_2 - K_1)\frac{\bar{p}_0 - \bar{p}_1}{\bar{p}_2 - \bar{p}_1} \tag{32}$$

This requires to solve the linear Stokes-like system at each time step 3 times. We can also add K to the unknowns of the Stokes-like linear system and add $\int_{\Gamma_{out}} p = |\Gamma_{out}|p_0$ to the equations; we used this second solution in the numerical tests because it is much less computer intensive.

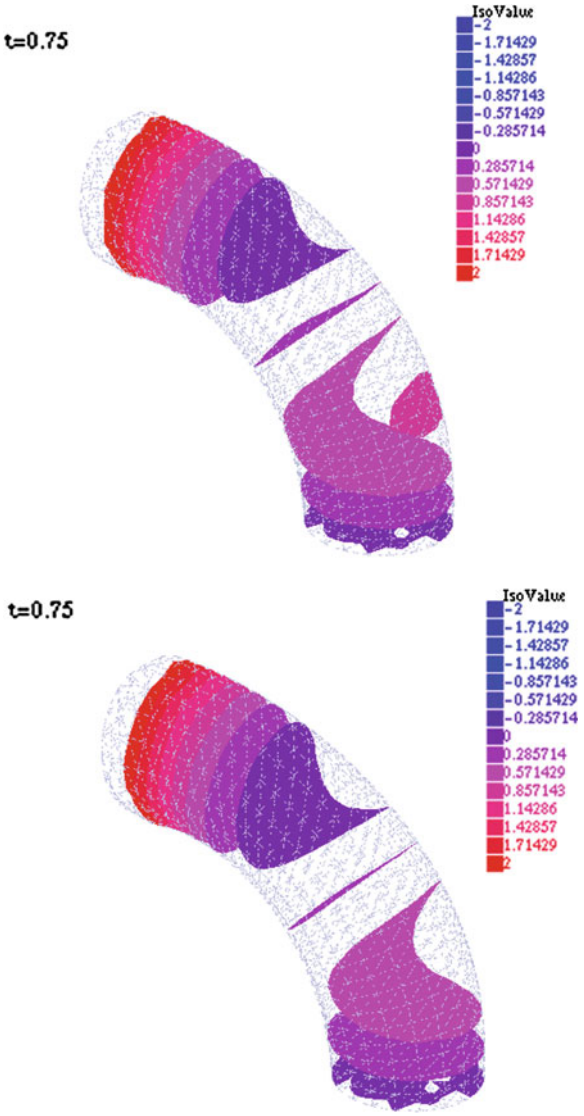

Fig. 2 *Left* surface of equal pressure at $t = 0.75$ computed by solving Problem 1 with $P^2 - P^1 - P^1$ elements and a penalization of the condition $u \times n = 0$. *Right* same as *left* but with Problem 2 and a $P^2 - P^1$ element

The idea is tested numerically on a quarter of a 2D-torus with radii 0.6 and 1 with $\nu = 0.002$ and a pressure drop equal to $\cos(t) + \cos(3t),\ t \in (0, 25)$. The PML viscosity is $\nu_1 = 0.2$. A PML region is added to both ends of the tube. Results are shown on Fig. 4.

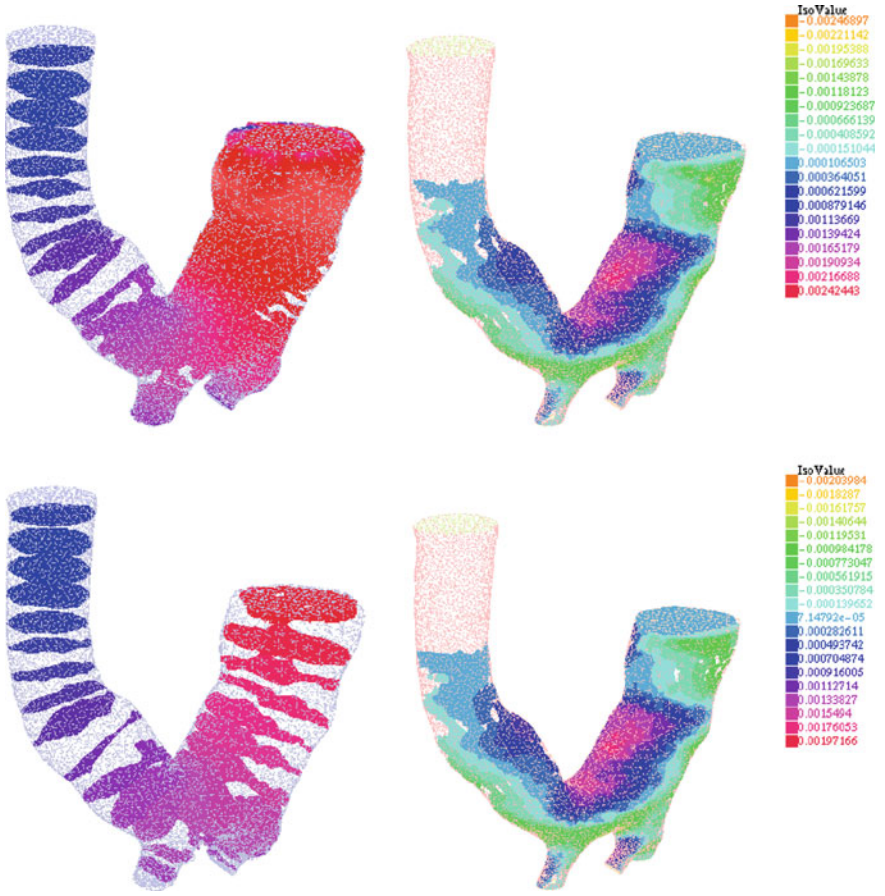

Fig. 3 Computation of $[u, p]$ for Problems 1 & 2 for a portion of an oarta (shown *upside down*). *Top* with Problem 1. the pressure is shown at $t = 0.8$ on the *left* on a geometry which has changed by η. On the *right* the third component of the velocity w is shown on the fixed geometry. *Bottom* same for Problem 2

The results look very different and that is because both computations do not have the same inflow and outflow conditions on the original inflow/outflow boundaries. In one case the pressure is imposed pointwise with $u \times n = 0$, in the PML case the mean pressure is imposed and no conditions are imposed on the velocity but parabolic velocity is imposed on the inflow/outflow of the PML boundaries.

The method will be tested in 3D and reported in a future publication.

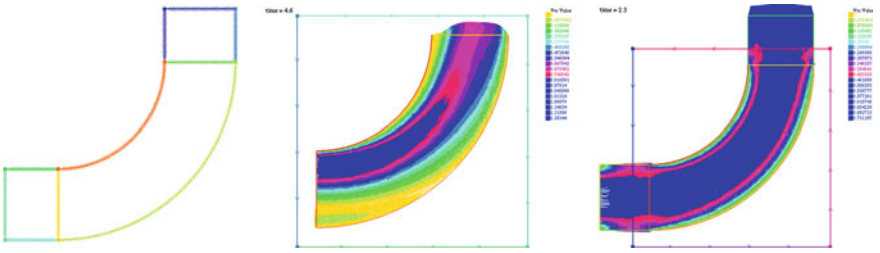

Fig. 4 *Left* Geometry for the flow with two PML regions added. *Center* the velocity vectors computed without the PML; notice the back flow in the *yellow* region. *Right* the same flow (velocity vectors) computed with the two PML regions. The pressure drop from the two inner boundaries (corresponding to the *top* and *left* boundaries of the geometry on the *center* figure) are the same as in the *center* figure

7 Conclusion

In this article we have presented problems and solutions encountered with fluid-structure interactions when a middle solution is seeked: neither the full problem with moving geometries because it is too expensive, nor rigid walls because it is not precise enough and it doesn't give the geometrical deformation.

The solution adopted here is to delay the geometrical deformations to the graphic diplay only. But in doing so we have to work with the Navier-Stokes equations with unusual boundary conditons which require unusual finite element discretizations.

For these intermediary problems we have shown that it is important to preserve energy. Furthermore we can choose either to match exactly the normal component of the solid and fluid normal stress tensor or to match approximately the 3 componenets of the normal stresses by relaxing slightly the no slip condition.

In all cases the problem of back flows in the pulsating cases remains. We have suggested a possible solution and made some preliminary tests.

References

1. Boffi D, Gastaldi L (2003) A fem for the immersed boundary method. Comput Struct 81:491–501
2. Deparis S, Fernandez MA, Formaggia L (2003) Acceleration of a fixed point algorithm for fluid-structure interaction using transpiration conditions. ESAIM:M2AN 37(4):601–616
3. Fernandez M (2013) Incremental displacement-correction schemes for incompressible fluid-structure interaction. Numer Math 123:21–65
4. Formaggia L, Gerbeau JF, Nobile F, Quarteroni A (2001) On the coupling of 3d and 1d navier-stokes equations for flow problems in compliant vessels. Comput Methods Appl Mech Eng 191:561–582
5. Formaggia L, Quarteroni A, Veneziani A (eds) (2009) Cardiovasuclar mathematics, MS and A series. Springer, Milano

6. Girault V (1988) Incompressible finite element methods for Navier-Stokes equations with nonstandard boundary conditions in R^3. Math Comp 51(183):55–74
7. Gonzalez O (2000) Exact energy and momentum conserving algorithms for general models in nonlinear elasticity. Comput Methods Appl Mech Eng 190:1763–1783
8. Gonzalez O, Simo JC (1996) On the stability of symplectic and energy-momentum algorithms for nonlinear Hamiltonian systems with symmetry. Comput Methods Appl Mech Eng 134:197–222
9. Hu Fang Q, Li XD, Lin DK (2008) Absorbing boundary conditions for nonlinear euler and navier-stokes equations based on the perfectly matched layer technique. J Comp Phys 227:4398–4424
10. Le Tallec P (2001) Fluid structure interaction with large structural displacements. Comput Methods Appl Mech Eng 190:3039–3067
11. Nobile F, Vergana C (2008) An effective fluid-structure interaction formulation for vascular dynamics by generalized robin conditions. SIAM J Sci Comp 30(2):731–763
12. Peskin C, McQueen D (1989) A three dimensional computational method for blood flow in the hearth-i. immersed elastic fibers in a viscous incompressible fluid. J Comput Phys 81:372–405
13. Peskin C (2002) The immersed boundary method. Acta Numerica 11:479–517
14. Pichon KG, Pironneau O (2014) Pressure boundary conditions for blood flows. Applied Math Conf in honnor of L. Tartar. Proc published in AIMS journal (to appear)
15. Pironneau O (1986) Conditions aux limites sur la pression pour les équations de Stokes et de Navier-Stokes. C R Acad Sci Paris Sér I Math 303(9):403–406
16. Pironneau O (1989) Finite element methods for fluids. Wiley, New York
17. Thiriet M (2011) Biomathematical and biomechanical modeling of the circulatory and ventilatory systems. Control of cell fate in the circulatory and ventilatory systems, vol 2. Springer, New York
18. Usabiaga F, Bell J, Buscalioni R, Donev A, Fai T, Griffith B, Peskin C (2012) Staggered schemes for fluctuating hydrodynamics. Multiscale Model Sim 10:1369–1408
19. Vignon-Clementel I, Figueroa A, Jansen K, Taylor CA (2006) Outflow boundary conditions for three-dimensional finite element modeling of blood flow and pressure in arteries. Comput Methods Appl Mech Eng 195:3776–3796